Egypt. J. Chem. **Vol. 67,** No. 10 pp. 383- 388 (2024)

Egyptian Journal of Chemistry

http://ejchem.journals.ekb.eg/

Investigation and Characterization of Physical Properties and Phonon modes of ZnO/ PVA/PANI for Photonic Crystals application.

Eman H. Ahmed [1] and Magdy M.H. Ayoub[1]

[1]Polymers and Pigments Department, Chemical industries research institute, advanced materials and nanotechnology group, National Research Centre (NRC), Egypt, Dokki 12622, Cairo, Egypt

Abstract

For potential photonic crystals fabrication, studying the physical and chemical features of zinc oxide doped with polyvinyl alcohol and polyaniline ZnO/PVA/PANI as nanocomposite to ensure its conduction level was the main goal of this work. The prepared nanocomposites of ZnO/PVA/PANI were obtained by in-situ chemical oxidation method using solution casting as coating technique. ZnO/PVA/PANI nanostructured composite was initially checked structurally, morphologically and optically. Field emission high resolution scanning electron microscopy (FEHRSEM) and FTIR were utilized for nanostructure morphological confirmation and structure investigation. The interaction of ZnO and the polymeric blend displaying the role of the incorporation of the semiconducting ZnO affecting the structure and changing the optical absorbance of the PVA/PANI nanocomposite compared to pure counterpart. A number of diffraction peaks were visible in the hexagonal wurtzite phase of zinc oxide at 30.78°(100), 34.44°(002), 36.28°(101), 47.58°(102), 56.62°(110), and 62.00, indicating a strong intermolecular hydrogen link between ZnO and the PVA/PANI co-blend. In the Raman analysis, the longitudinal optical (LO) phonons, and various low and high phonon modes are clearly visible.

Keywords: Morphology, Nanocomposite, Phonon modes, Raman Spectra

1. Introduction

Because of their exceptional mechanical qualities, ease of production, and lightweight nature, optical materials are widely garnering more and more interest in both academic and industrial aspects. High index of refraction polymers with good optical absorbance could find use in potential optical devices [1-6], such as matamaterials [7, 8], organic light-emitting diodes [9-12], microlenses [13,14], image sensors [15, 16] and photonic crystals [17–24]. More precisely, photonic crystals can dramatically and enthrallingly alter our understanding of how light waves interact with the objects. It is the use of coatings with high and low refractive indices on mirrors and lenses. And as a result, the qualities and uses of photonic crystals have left us more and more in wonder to develop our understanding of the light technology. Consequently, a frequent parameter to significantly raise the refractive index of polymers is to incorporate chemical groups with high molar refraction and low molar volume. Pure PVA has some drawbacks that limit its application in industry, such as a low elastic modulus, poor abrasion resistance, and a significant creep issue [9-12]. These drawbacks cause pure PVA to fail early. Due to this, scientists have used a range of other polymers to form co-polymer block composites with improved properties [13]. The most often used conducting polymer is PANI, which can have quinoid, benzenoid, or even both types of structures [14-16]. When an n-type semiconductor, such as ZnO, is combined with a p-type polymer, such as PANI, a p-n junction is created, which lowers the rate of electron-hole recombination and prevents photocorrosion [17-20]. Additionally, PANI may function as a h+ acceptor and an e− donor [19]. In addition to being an inexpensive material, PANI exhibits good environmental stability and is simple to synthesis. ZnO nanostructure as an oxide material has drawn a lot of interest recently as an appropriate matrix for biomolecule binding. For this reason, the incorporation of ZnO nanostructures into PVA/PANI

*Corresponding author e-mail: eman_helmy111@yahoo.com.; (Eman H. Ahmed).
Receive Date: 11 July 2024, Revise Date: 13 August 2024, Accept Date: 18 August 2024
DOI: 10.21608/ejchem.2024.303448.9993
©2024 National Information and Documentation Center (NIDOC)

has incredibly influenced on the optical and photonic properties especially in sensors technology. The physicochemical analysis has generated a lot of interest because the electrochemical enzymatic sensors have dominated the practical market for photonic structures, bio-imaging and biosensors due to their excellent selectivity [9-10]. Based on these characteristics, modifying the nanoparticles of ZnO with polymeric materials, chemical compounds, and biomolecules can transform them into robust and biocompatible promising nanocomposites in several applications [14, 15]. Illustrating how the semiconducting ZnO's addition changed the PVA/PANI nanocomposite's optical absorbance and affected its structure in comparison to its pure counterpart is the novelty of the present work. Revealing the optical absorbance of ZnO/PVA/PANI altering the physicochemical Raman ability and the structural compatibility of this nanocomposite in photonic crystals is the basic goal of this study. Therefore, the future research development should demonstrate empirically that a microcavity super-sensitive ZnO/PVA/PANI as a 2D photonic crystal. Photonic crystal structures have been successfully employed in intelligent sensing, information transmission, and other fields because of their optimal light-interacting properties [19-20]. For instance, Xiao et al. [20] created an intelligent photonic crystal hydrogel material in which the photonic crystal array is fixed in a polyvinyl alcohol (PVA) hydrogel matrix and the difraction wavelengths can be effectively adjusted in the visible region. This material can be used for real-time monitoring, through physical crosslinking.

2.1. Materials and methodology

Polyvinyl alcohol (PVA) (M.wt. 125,000), ethanol and Polyaniline (average Mw 10,000), were purchased from Merck, (Germany) and Loba Chemie (India), respectively. Zinc oxide nanoparticles (99%), <100 nm particle size (TEM), ≤40 nm avg. part. size (APS), 20 wt. % in H_2O were purchased from Sigma Aldrich. 0.1% of ZnO nanoparticles were dispersed in 50 ml DI water and allowed to disperse in an ultrasonic water bath for 30 min to ensure the homogeneous solution. 5 grams of PVA were dissolved in 100 milliliters of DI water to create PVA with a 5% concentration and then introducing 2% PANI solution to the former one. PANI solution can be dissolved in an aqueous solution of sulphuric acid with a concentration of 1%**.** The mixture was subsequently allowed to continued stirring for 5 hr at 70°C and coated using solution casting technique.

2.2. Substrate cleaning conditions

The plastic substrate has dimensions of 2.5 cm × 2.5 cm × 0.2 cm and allows for adjustable sensitivity settings. For controllable sensitivity conditions, the conductive plastic substrate must be cleaned before application. To remove any remaining salt from the surface, the substrates were ultrasonically cleaned in ethanol solution and de-ionized water over the course of 15 to 30 minutes. They were then allowed to dry in the air at ambient temperature, or roughly 25°C. To guarantee proper dispersion and uniformity, contaminants must be removed.

2.3. Characterizations

High sensitivity Raman microscope Senterra Bruker laser source 532 nm (Germany) with high wave number accuracy and permanent calibration was the defining feature of Raman spectroscopy. Using KBr pellets, the FTIR transmittance spectra were recorded using a Japanese-made JASCO FT-IR 6100. The ZnO/PVA/PANI nanocomposites' surface morphology was examined using a field emission scanning electron microscope (HRFESEM). Absorbance spectra were obtained using Jasco model V-570 UV/VIS/NIR spectrophotometer. The measurements were carried out in the wavelength range of 300 to 800 nm.

The opposite of transmittance, absorbance (A) indicates how much light the sample absorbed. Another name for it is "optical density." As a logarithmic function of T, absorbance is computed as follows:

$$A = \log_{10} (Io/I) \quad (1)$$

Where Io is the incident intensity, I is the transmitted intensity, and (A) is the absorption.

Given the symbol I, the intensity of the light entering the sample cell is also measured for that wavelength. A portion of the light has been absorbed by the sample if I is smaller than Io.

Results and discussion

As predicted, ZnO showed a prominent, small band at 465 cm^{-1}, which represented the high mode of the oxygen atoms in ZnO served as the band's origin due to the stretching frequency of Zn–O bonds which confirmed the presence of metal–oxide [37] as shown in Figure (1). Another sharp peak at 1801.1cm $^{-1}$, correspond to the standard peak of free PVA has been shifted to the lower for ZnO/PVA/PANI (b) indicating the interaction of PVA/PANI and ZnO. Prominent peaks, about 1436 cm-1 are ascribed to the bending of -CH and -OH, whereas approximately 2919 cm^{-1} are caused by the stretching vibrations of -CH and -CH_2 in ZnO/PVA nanocomposite [37] . It is clearly seen that the bands related to ZnO modes such as at 465 cm^{-1} slightly shifted towards a higher frequency and intensity. On the other hand, a broad band at 1614 cm^{-1} was detected as the quinoid unit band of PANI. A decrease in the physical conjugation of PVA/PANI and

the interaction between PVA/PANI and ZnO was suggested by shifts in the band of PVA chains [25]. The C–H bending in-plane of benzenoid or quinoid unit, C–N bending in-plane of benzenoid unit, and N=C=N stretching in quinoid units of polyaniline were identified as the vibration bands recorded at 1030 cm^{-1}, 1200 cm^{-1}, and 811 cm^{-1}, respectively which agreed as previously reported [26-29].

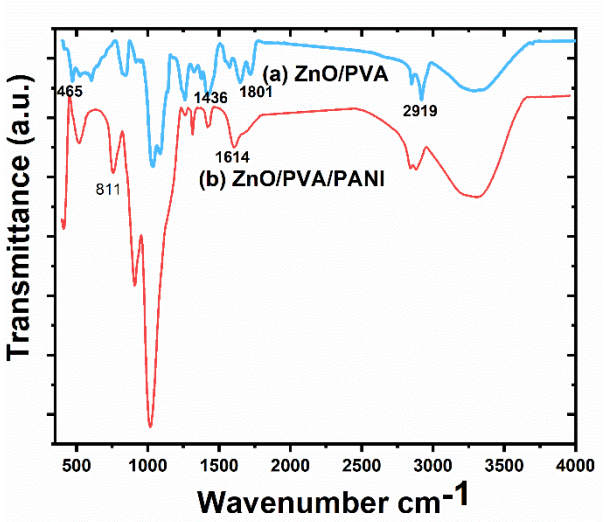

Figure (1) FTIR spectra of (a) ZnO/PVA and (b) ZnO/PVA/PANI

ZnO's SEM picture showed a variety of polyhedral forms as displayed in Figure (2). Because of the incorporation of PVA/PANI concentration, the observed change in ZnO morphology appeared as an increase in aggregate size. This result verified that PANI and ZnO were present in ZnO/PVA/PANI nanocomposite sample. PANI polymer chains were visible in the SEM images of the composite, either partially surrounding the ZnO particles or extending into their perimeter. Diffusion may be the cause of some nanoparticles that are coupled to one another. Some enlarged ZnO nanoparticles adhered to one another.

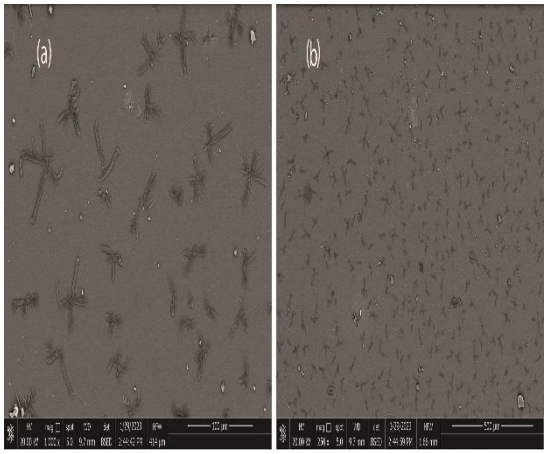

Figure (2) SEM images of ZnO/PVA/PANI at different magnifications (a) x 1000 and (b) x 250

The obtained FESEM images were used to investigate the nanostructure formation at two different magnifications, 1000 X and 250 X, respectively. A good dispersion of the ZnO particles into PVA/PANI was abundantly evident that the new nano-composite was homogeneously distributed.

The absorption spectra results were shown in Figure (3). Since the interaction of PVA/PANI was carried out physically in different directions, creating several morphologies after the interaction with ZnO nanostructure. This could be explained in the optical absorbance as a slight shift in the peak at 340 nm was indicating the possibility of some intermediate structure creation as a result of the reaction between ZnO and PVA/PANI. The absorption spectra were measured from 300 up to 1600 nm excitation wavelength. Different absorption peaks have varied intensities and positions as the reported data in this work due to the interaction of ZnO and PVA/PANI system [30].

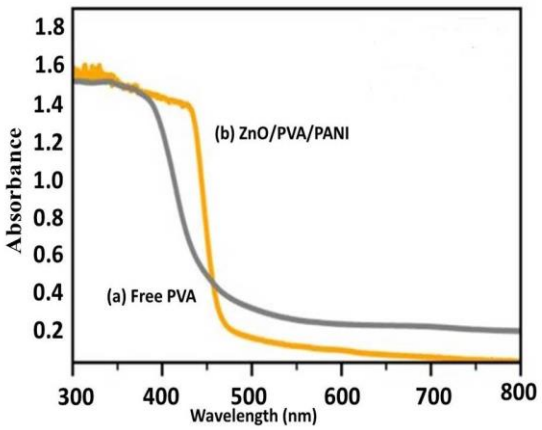

Figure (3) Absorption spectra of (a) Free PVA and (b) ZnO/PVA/PANI

The Raman spectra of ZnO/PVA/PANI are displayed in Figure (4). According to the group theory, there are three sets of central optical phonons, one of which are Raman active and correspond to the transverse optical (TO) phonons, one of which are longitudinal optical (LO) phonons, and the other are low and high phonon modes. The phonon mode, which is characteristic of the wurtzite phase in particular, is most noticeable around 438 to 600 cm^{-1}[31-34]. The low phonon mode is characterized by a peak close to 465 cm^{-1} in FTIR [30]. The second and third Raman regions which come from the zone boundary phonon, which emerged around 1200 and 1750cm^{-1} explaining the growth in different directions after the interaction with PVA/PANI. Consequently, the polar phonons in the wurtzite structure induce anisotropy in the macroscopic electric field resulting (TO) mode at a 533 cm^{-1} center. In

addition to other signature peaks which are located at 578 cm^{-1} and 750 cm^{-1} [38]. Since the various morphologies of the nanostructures have a distinct morphology which may cause increase in the 2450 cm^{-1} of the pure PANI sample. Two prominent peaks about 1436 cm^{-1} and approximately 2919 cm^{-1} are ascribed to the bending of -CH and -OH, whereas are caused by the stretching vibrations of -CH and -CH_2 in ZnO/PVA/PANI sample.

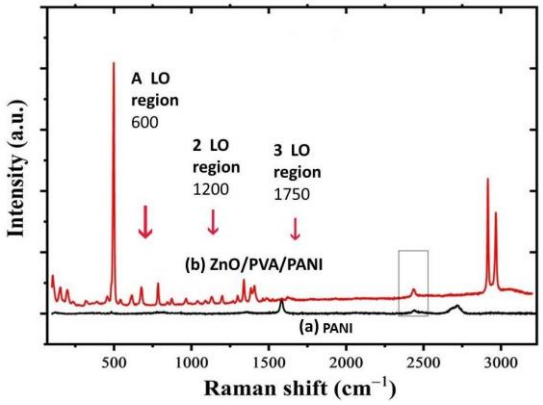

Figure (4) RAMAN spectra of (a) PANI and (b) ZnO /PVA/PANI, illustrating A LO, 2LO and 3 LO regions

Several diffraction peaks can be seen in the XRD as shown in Figure (5) at the following two theta: 30.78°(100), 34.44°(002), 36.28°(101), 47.58°(102), 56.62°(110) and 62.00°(103) due to the hexagonal wurtzite phase of zinc oxide. Every diffraction peak matches perfectly with ZnO's hexagonal wurtzite crystal structure (JCPDS 89–1397) [30-34]. In the ZnO/PVA/PANI composite we can find the characteristic peaks which correspond to the main crystalline region emerged after the interaction with PVA/PANI. It could be revealed due to the oxygen-containing groups in the ZnO and the hydroxyl groups in the PVA matrix established hydrogen bonds, which led to the total dispersion of the ZnO particles in the PVA matrix. A characteristic intense peak was seen in the PVA, and the reflection plane of the crystalline PVA could be matched by the PVA/ZnO nanocomposites at the scattering angle of 2θ = ~19.9° in relation to the 'd' spacing of 4.57 Å [30-34]. The strong intermolecular hydrogen bonding that exists between PVA, ZnO and PANI chains is responsible for the crystalline structure of ZnO/PVA/PANI nanocomposite.

However, compared to pure PANI in the literature, it is clear that ZnO/PVA/PANI showed a greater improvement in the PANI's crystallinity revealing a number of peaks at appropriate intensities due to the repeating benzenoid and quinoid rings in PANI chains, the peak diffracted at an angle of 2θ = 10.30◦ (d spacing of 4.366 Å and 3.520 Å, respectively) revealed the improvement crystallinity of PANI. [35-36].

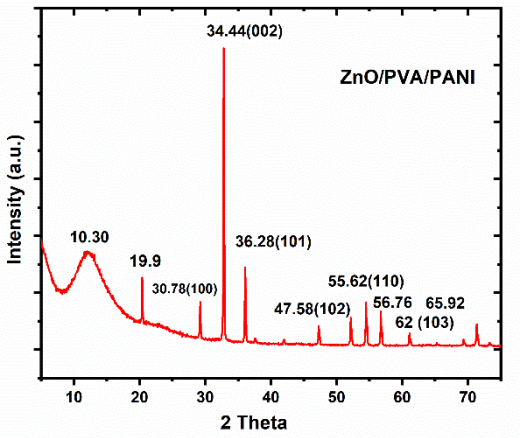

Figure (5) XRD of of ZnO /PVA/PANI nanocomposite

Conclusion

The aim of this study is to analyze the chemical structure and the physical composition of ZnO nanoparticles embedded PVA/PANI nanocomposite to be introduced in photonic crystals application. XRD, SEM, FTIR and Raman spectra were used for altering the successful interaction between ZnO and polymeric chains. The phonon mode, which is characteristic of the Wurtzite phase is obviously noticeable around 438 to 600 cm^{-1}. The transverse optical (TO) phonons, longitudinal optical (LO) phonons and the other are low and high phonon modes are clearly observed in the Raman analyzing. The Wurtzite phase matches perfectly with ZnO's hexagonal crystal structure as shown in the diffraction peak card number (JCPDS 89–1397).

CRediT authorship contribution statement

Eman H. Ahmed: Conceptualization, Methodology, Graphs and Investigations, Analysis, Writing original draft, Data Curation, Funding acquisition, Review and Editing **Magdy M.H. Ayoub:** Review & Editing**,** Funding acquisition.

Conflict of Interests

The authors declare that they have no conflict of interest

Funding:

Self-funding

Data availability

The data that support the findings of this study are available frm the corresponding author upon request.

References:

1. K. Demssie Dejen, E. Amare Zereffa, H C Ananda Murthy, and A. Merga, Synthesis of ZnO and ZnO/PVA nanocomposite using aqueous Moringa Oleifeira leaf extract template: antibacterial and

electrochemical activities, Rev. Adv. Mater. Sci. (2020) 59:464–476
2. A.Palumbo, L. ZQ, Yang EH. Trends on carbon nanotube-based flexible and wearable sensors via electrochemical and mechanical stimuli: a review. IEEE Sens J. (2022), 22:20102–25
3. K. S Hemalatha, K. Rukmani, N. Suriyamurthy, and B. M. Nagabhushana. Synthesis, characterization and optical properties of hybrid PVA–ZnO nanocomposite: A composition dependent study. Materials Research Bulletin (2014) 51, 2014, 438–446.
4. N.Matinise , X. G. Fuku, K. Kaviyarasu, N. Mayedwa, and M. Maaza. ZnO nanoparticles via Moringa oleifera green synthesis: Physical properties & mechanism of formation. Appl. Surf. Sci. (2017) 406, 339-347
5. K. Ali, M. Mohammed, N.K. Sabah, and AL-Thomir. Preparation and characterization of antimicrobial PVA/ZnO nanocomposite for biomaterial applications. Journal of University of Babylon, Eng. Sci. (2018) 26, 286–294.
6. A. Akhavan, F. Khoylou, E. Ataeivarjovi, Preparation and characterization of gamma irradiated Starch/PVA/ZnO nanocomposite films. Radiat. Phys. Chem. (2017) 138, 49–53
7. K. K.Deepak, .J. Suraj, K. K. Pawan, N.Vijayan, and B. Shaibal. Synthesis, Characterization, and Studies of PVA/Co-Doped ZnO Nanocomposite Films. Int. J. of Green Nanotech. (2012) 4, 408–416.
8. Q. K Muhammad, K. Davood, N. Nazish, S. Amir, H.Tanveer, K.Zeeshan, Preparation and characterizations of multifunctional PVA/ZnO nanofibers composite membranes for surgical gown application. J. of Mater. Research and Tech. (2019) 8, 1328-1334.
9. L. Jian, Z. Qun, X. Minjing, W. Changzhu, and L. Ping. Antimicrobial eflcacy and cell adhesion inhibition of in situ synthesized ZnO nanoparticles/polyvinyl alcohol nanofibrous membranes. Advanc. in Condensed Matter Physics (2016) 4, 1- 9
10. A Ngamaroonchote, Y Sanguansap, T Wutikhun, K. Karn Orachai, Highly branched gold copper nanostructures for non -enzymatic specific detection of glucose and hydrogen peroxide. Microchim Acta. (2020),32,17-27
11. D Rodrigues, A Barbosa, R Rebelo, I. Kwon, R. Reis, V. Correlo. Skin- integrated wearable systems and implantable biosensors: a comprehensive review. Biosensors (Basel). 2020.
12. V.Eskizeybek, F. Sarı , H.Gülce, A Gülce., A. Avcı, Preparation of the new polyaniline/ZnO nanocomposite and its photocatalytic activity for degradation of methylene blue and malachite green dyes under UV and natural sun lights irradiations. Appl. Catal. B Environ. (2012), 119, 197–206.
13. V.Gilja, I.Vrban, V. Mandic, M.Zic; Z.Hrnjak Murgic, Preparation of a PANI/ZnO composite for efficient photocatalytic degradation of acid blue. Polymer (2018), 10, 940.
14. R.Nosrati, A. Olad, R. Maramifar, Degradation of ampicillin antibiotic in aqueous solution by ZnO/polyaniline nanocomposite as photocatalyst under sunlight irradiation. Environ. Sci. Pollut. Res. Int. (2012) 19, 2291–2299.
15. M.Nowakowsk, K. Szczubiałka, Photoactive polymeric and hybrid systems for photocatalytic degradation of water pollutants. Polym. Degrad. Stab. (2017) 145, 120–141.
16. U. Riaz, S.M Ashraf, Kashyap, J. Enhancement of photocatalytic properties of transitional metal oxides using conducting polymers: A mini review. Mater. Res. Bull. (2015), 71, 75–90.
17. X. Jin, G.Liu, C.Bao, M.Chen, Q.Huang, Improved stability and dispersity of ZnO@PANI nanocomposites aqueous suspension. Appl. Organomet. Chem. (2018) 32, 4411.
18. c Radoiˇci´, M. Šaponji´c, Z. Jankovi´c, I.A. Ciri´c Marjanovi´c, G. Ahrenkielc, S.P. ´ Comor, M.I. Improvements to the photocatalytic ˇ efficiency of polyaniline modified TiO2 nanoparticles. Appl. Catal. B Environ. (2013)136, 133–139.
19. M R Lee, P M Fauchet. Two-dimensional silicon photonic crystal based biosensing platform for protein detection. Optics Exp., 2007, 15(8): 4530-0.
20. F Xiao, Y Sun, W Du, et al. Smart photonic crystal hydrogel material for uranyl ion monitoring and removal in water. Advanced Functional Materials, (2017), 27(42): 1702147.
21. C. Pina-Hernandez, A. Koshelev, L. Digianantonio, Printable Planar Lightwave circuits with a high refractive index, Nanotechnology (2014) ,25, 325302
22. R. Betancur, P. Romero-Gomez, A. Martinez-Otero, Transparent polymer solar cells employing a layered light Trapping architecture, Nat. Photonics 7 (2013) 995.
23 C. Pina-Hernandez, V. Lacatena, G. Calafiore, A route for fabricating printable photonic devices with sub-10 nm resolution, Nanotechnology 24 (2013) 065301.
24. G. A.Elham, H. F. Mohammad, S. Nasser, K. Mehdi, and M. Parisa. Preparation and Characterization of PVA /ZnO Nanocomposite. Journal of Food Processing and Preservation, (2015), 39, 1442–1451
25. O. G. Abdullah, and S. A. Saleem. Effect of copper sulfide nanoparticles on the optical and electrical

behavior of Poly (vinyl alcohol) films. Journal of Elect. Materials, (2016) 45, (11), 5910–5920.
26. S. Bera , H Khan, I.Biswas, S.Jana, Polyaniline hybridized surface defective ZnO nanorods with long-term stable photoelectro- chemical activity. Appl. Surf. Sci. (2016), 383, 165–176.
27. M. Dhingra, S. Shrivastava; P. Senthil Kumar; Annapoorni, S. Polyaniline mediated enhancement in band gap emission of zinc oxide. Compos. B Eng. (2013) 45, 1515–1520.
28. Z. Pei, L.Ding, M Lu., Z.Fan, S.Weng; J.Hu, P.Liu, Synergistic effect in polyaniline-hybrid defective ZnO with enhanced photocatalytic activity and stability. J. Phys. Chem. C (2014)118, 9570–9577.
29. S.Tao, B.Hong , Z. Kerong An infrared and Raman spectroscopic study of polyanilines co-doped with metal ions and H+. Spectrochim. Acta A Mol. Biomol. Spectrosc. 2007, 66, 1364–1368.
30. A. Gupta, V. Deoram Nandanwar , R. Sanjay Dhakate, Electrospun self-assembled ZnO nanofibers structures for photocatalytic activity in natural solar radiations to degrade acid fuchsin dye, Adv. Mater. Lett. (2015) 6(8), 706-710
31. E. H. Ahmed, M. M. H. Ayoub, A. A. Ward, Dielectric properties of PANI-PEG nanocomposites filled with silica media for antistatic applications, Polymers Advanc. Tech, (2024) ,35: 6315.
32. V F Chernow, H Alaeian, J A Dionne, Polymer lattices as mechanically tunable 3-dimensional photonic crystals operating in the infrared. Appl. Physics Letters (2015), 107(10):101905
33. W S Fegadolli, N Pavarelli, P O Brien, thermally controllable silicon photonic crystal nanobeam cavity without surface cladding for sensing applications. ACS Photonics, (2015), 2(4): 470-474
34. A. Ali Rahma, E. M.Ezzo, S. A. Hassan, Magda. A. El kherbawi and Amira. S. Hassan, ZnO Nanoparticles as an Efficient, Heterogeneous and Ecofriendly adsorbent for Pollutant Dyes Removal, Egypt. J. Chem. (2023) 66, 13, 1749 - 1757
35. M.Š´cepanovi´c,M.Gruji´c-Broj˘cin, K.Vojisavljevi´c, S.Bernik, T. Sre´ckovi´, Raman study of structural disorder in ZnO nanopowders. J. Raman Spectrosc (2010) 41, 914–921.
36. L.Shi, X.Wang, L.Lu, X Yang, X. Wu Preparation of TiO2/polyaniline nanocomposite from a lyotropic liquid crystalline solution. Synth. Met. (2009)159, 2525–2529
37. D.Sreetama and N. G. Bichitra. Characterization of ZnO nanoparticles grown in presence of Folic acid template. Journal of Nanobiotechnology (2012), 29, 10–29
38. Y.C. Liu , Y.M. Lu , J.Y. Zhang , D.Z. Shen , X.W. Fan, Photoluminescence and Raman behaviors of ZnO nanostructures with different morphologies, Journal of Crys. Growth (2006) 289, (1), 55-58.